VIENNA UNIVERSITY OF TECHNOLOGY
DEPARTMENT OF GEODESY
AND GEOINFORMATION

GEOWEB Training course on modern geodetic topics
Mostar, Bosnia and Herzegovina
October 16, 2017

Modeling tropospheric delays in space geodetic techniques

Daniel Landskron

Contents

2

Bild 2

D10 I will shortly introduce some physics behing tropospheric delays and then talk about fundamentals of troposphere modeling, sorry for those who already know this

D.Landskron; 2017-10-03

1. Fundamentals

3

Troposphere

- Troposphere delays: strictly speaking delays in the neutral atmosphere (up to 100 km) D8
- Radio signals are delayed and bent due to interaction with gases and water particles => refractivity
- Essentially no frequency dependence across microwave regime D1
- Small frequency dependence for optical techniques (Satellite Laser Ranging)

4

Bild 4

D1 unlike the ionosphere, which is indeed frequency dependent and whose effect can therefore be eliminated through measuring in two frequency bands
D.Landskron; 2017-10-03

D8 the neutral atmosphere is defined as that part of the atmosphere which is non-ionized, contrary to the ionosphere
whereas the troposphere is that part of the atmosphere below the first temperature inversion.

However, spatially those two coincide, why the sloppy term "troposphere" is used
D.Landskron; 2017-10-03

Refractivity

- Strictly speaking, refractivity is a complex number

$$N = N_0 + N'(\nu) - i\,N''(\nu)$$ D2

- Real part: causes refraction and propagation delays
- Imaginary part: causes absorption; important for water vapour radiometers D3

D2

5

Refractivity of microwaves

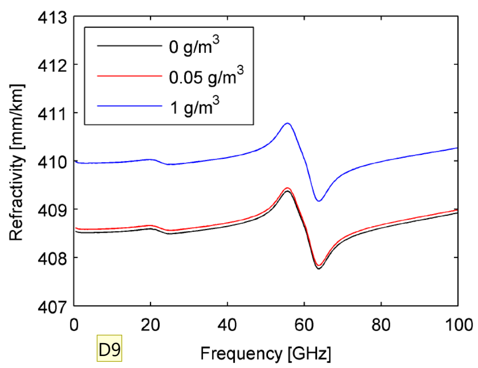

D9

Figure 21: The total refractivity as function of frequency. The total pressure is 1013 hPa, the temperature 300 K, and the relative humidity is 100 %. Three different cases are shown corresponding to different concentrations of liquid water: 0 g/m^3, 0.05 g/m^3, and 1 g/m^3

6

Bild 5

D3 as water vapour radiometers are capable of measuring the delay of a signal arising from water vapor
D.Landskron; 2017-10-03

D2 but in the following we only consider the real part, that is, we neglect the attenuation of the signal
D.Landskron; 2017-10-03

D2 this term here (v) is frequency
Daniel; 2017-10-12

Bild 6

D9 as the frequencies of GNSS lie slightly above 1 GHz and VLBI below 10 GHz as well, we can consider the refractivity to be frequency independent (visible through the straight line)

in the optical range, this is different
D.Landskron; 2017-10-03

Refractivity of microwaves

Distinguished between a hydrostatic part and a wet part

$$N = k_1 \frac{R}{M_d}\rho + k_2' \frac{p_w}{T} Z_w^{-1} + k_3 \frac{p_w}{T^2} Z_w^{-1} = N_h + N_w$$

hydrostatic — wet

D1

$$k_2' = k_2 - k_1 \frac{M_w}{M_d}$$

7

Refractivity of microwaves

Wet part: surface values not representative for the upper air conditions

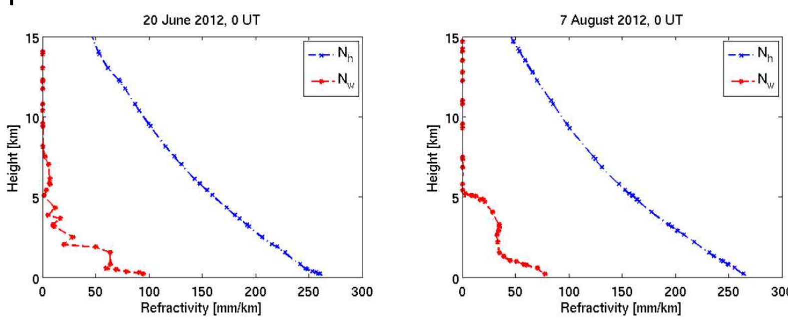

Figure 22: Examples of vertical profiles of the hydrostatic and wet refractivity. The profiles are calulated using radiosonde data from Vienna, Austria.

8

Bild 7

D1 there would be a further term for liquid water, but it is not contained in this formula
Daniel; 2017-10-12

Optical refractivity of moist air

- k_3 can be ignored; Wet part smaller D11
- Small frequency-dependency

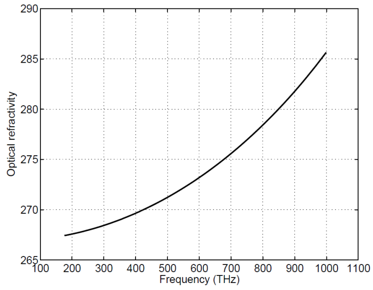

Figure 23: The total optical refractivity as function of frequency. The total pressure is 1013 hPa, the Temperature 300 K, and the relative humidity is 100%.

9

2. Modeling delays in the troposphere

10

Bild 9

D11 say: the wet part is approximately 70 times smaller
D.Landskron; 2017-10-03

D3

Definition of path delay in the neutral atmosphere

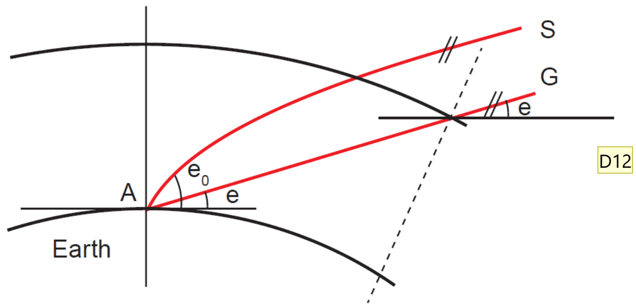

D12

Figure 24: Path taken by a signal through the atmosphere. The signal will take the path with the shortest propagation time (S). Since the signal propagates slower in the atmosphere than in vacuum, the geometrical length of S will be larger than the straight path G

Bending effect [S - G] about 0.2 m at 5° elevation (added to the hydrostatic mapping function)

11

Delays in zenith direction

- Zenith hydrostatic delay
  - Ca. 2.3 m at sea level D13
  - Can be determined very accurately from *p* (mm-accuracy) D14 + Saastamoinen (1972)

- Zenith wet delay
  - Ca. 0.05 - 0.4 m at sea level
  - Rule of thumb: $\Delta L_w^z \, [\mathrm{cm}] \approx p_{w0} \, [\mathrm{hPa}]$
  - Can only be approximated from surface data GPT2/GPT3 + Askne & Nordius (1987) D16

12

Bild 11

D12 this is a simplified graph how the bending looks like
D.Landskron; 2017-10-03

D3 Das Beispiel mit dem Lifesaver bringen
Daniel; 2017-10-14

Bild 12

D13 and decreases with increasing height
D.Landskron; 2017-10-03

D14 approximate station position is also needed
D.Landskron; 2017-10-03

D16 because the wet refractivity is highly variable in the vertical column
D.Landskron; 2017-10-03

Pressure values

- Simple empirical models like Berg (1948) and Hopfield (1969)

$$p = 1013.25 \cdot (1 - 0.0000226h)^{5.225}$$

$$p = 1013.25 \cdot \left(\frac{T_k - \alpha h}{T_k}\right)^{\frac{g}{R_d \alpha}}$$

- More sophisticated models like
  - UNB3m (5 latitude bands, annual with fixed phase)
  - GPT (9x9 spherical harmonics, annual with fixed phase)
  - GPT2/GPT3 (5°x5° or 1°x1° grid, annual + semi-annual terms)

13

Pressure values

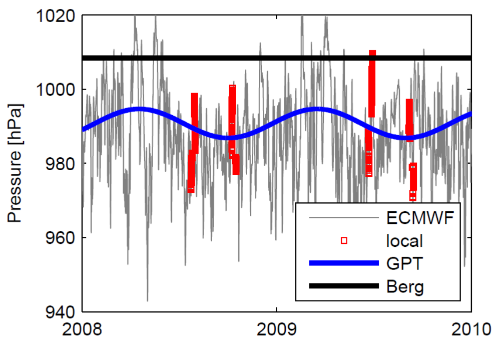

Figure 25: Pressure values for station O'Higgins in Antarctica from the ECMWF (grey line), local pressure recordings at the radio telescope (red squares), GPT (blue line), and pressure determined with the model by Berg (1948) (black line)

14

Precipitable water

- Integrated water vapour IWV in kg/m^2

$$IWV = \frac{10^6 ZWD}{\left[k'_2 + \frac{k_3}{T_m}\right] R_v}$$

- Precipitable water PW in m

$$PW = \frac{IWV}{\rho_l}$$

- PW is approximately 1/6 of the zenith wet delay

15

Water vapor comparison

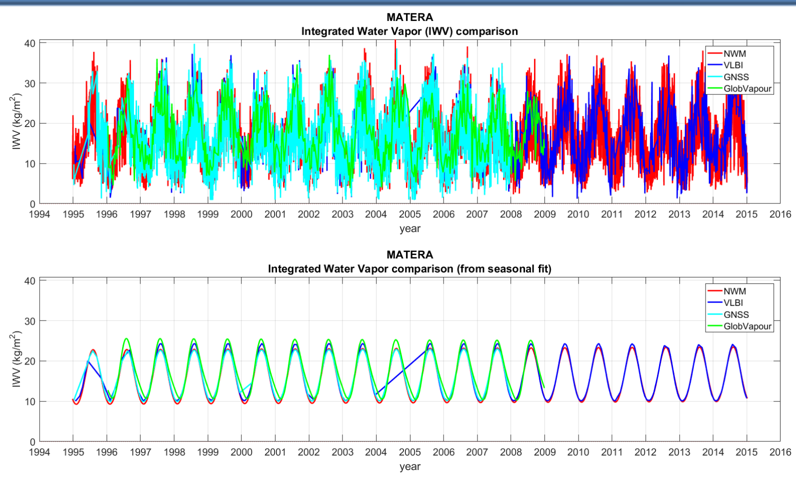

Comparison of IWV for station **MATERA**

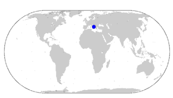

16

Modeling troposphere delays

Assuming Azimuthal Symmetry:

$$\Delta L(e) = \Delta L_h^z \cdot mf_h(e) + \Delta L_w^z \cdot mf_w(e)$$

- *ΔL(e)*: total delay dependent on elevation
- ΔL^z_h: hydrostatic delay in zenith direction; can be modeled a priori
- ΔL^z_w: wet delay in zenith direction; approximated or estimated in data analysis
- *mf(e)*: mapping function ($mf_h > mf_w$)

17

Mapping functions

- Mapping function not perfectly known
- Errors via correlations also in station heights (and clocks)
- Low elevations necessary to de-correlate heights, clocks, and zenith delays
- Rule of thumb: the station height error is about 1/5 of the delay error at 5°elevation (if cutoff angle is 5°)

18

Mapping functions

- Continued fraction form (Herring, 1992)

$$mf(e) = \frac{1 + \frac{a}{1 + \frac{b}{1 + c}}}{\sin(e) + \frac{a}{\sin(e) + \frac{b}{\sin(e) + c}}}$$

19

Mapping function models

- Saastamoinen (1972), Chao (1974), CfA2.2 (Davis et al., 1985), ...
- **MTT**: MIT Temperature mapping functions (Herring, 1992)
- **NWF**: New Mapping Functions (Niell, 1996)
- **IMF**: Isobaric Mapping Functions (Niell, 2000)
- **VMF**: Vienna Mapping Functions (Böhm et al., 2006)
- **GMF**: Global Mapping Functions (Böhm et al., 2006)
- **GPT2/GPT2w** (Lagler et al., 2013, Böhm et al., 2015)
- **VMF3/GPT3** (Landskron and Böhm, 2017)

20

Modeling troposphere delays

Assuming Azimuthal Asymmetry:

$$\Delta L(a,e) = \Delta L_h^z \cdot mf_h(e) + \Delta L_w^z \cdot mf_w(e) + mf_g(e) \cdot (G_n \cos a + G_e \sin \mathrm{a})$$

- $\Delta L(a,e)$: total delay dependent on azimuth and elevation (m)
- ΔL^z: delay in zenith direction (m)
- $mf(e)$: mapping function
- G_n: north gradient (m)
- G_e: east gradient (m)

21

Horizontal gradients

- Horizontal gradients due to:
  - Atmospheric bulge
  - Weather fronts
  - Coastal conditions
- Chen and Herring (1997)

$$\Delta L(a,e) = \Delta L_0(e) + mf_g(e)(G_n \cos(a) + G_e \sin(a))$$

$$mf_g(e) = \frac{1}{\sin(e)\tan(e) + C}$$

$C_h = 0.0031$, $C_w = 0.0007$

- Typical gradient: 1 mm (corresponds to 0.1 m delay at 5° elevation)

22

Horizontal gradients

- Correspond to tilting of the mapping function

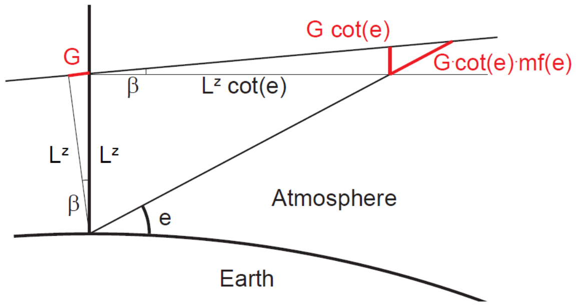

Figure 33: Tilting of the mapping function by the angle β assuming a horizontally stratified atmosphere

23

Horizontal gradient models

Gradients are either estimated in the analysis or they are determined from external data (e.g. NWM)

<u>A priori models:</u>

- **DAO** (MacMillan and Ma, 1997)
- **LHG** (Böhm and Schuh, 2007)
- **APG** (Böhm et al., 2013)
- **GRAD** (Landskron et al., 2016)
- **GPT3** (Landskron et al., 2017)

24

Ray-tracing

- To find the ray-path from the source to the telescope (iterative calculation)
- Coupled differential equations need to be solved
- 1D, 2D or 3D ray-tracing
- Feasible for VLBI but probably not for GNSS
- Basis for most accurate mapping functions and gradient models (VMF series)

25

Ray-tracing

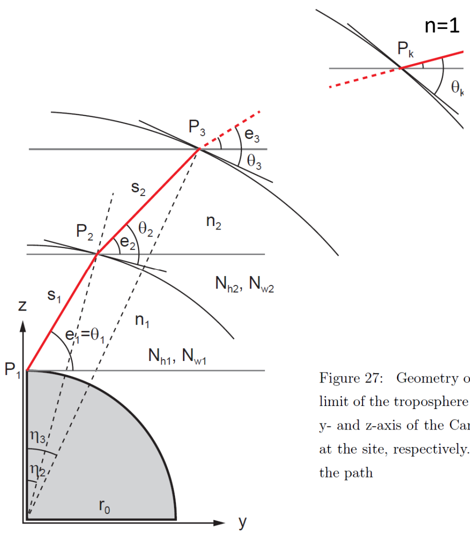

D18

Figure 27: Geometry of a 1D ray-tracing method, for a receiver located at P_1 and the upper limit of the troposphere at P_k. Points P_2 and P_3 show two sample points of the ray path. The y- and z-axis of the Cartesian coordinate system are parallel to horizon and zenith direction at the site, respectively. $S_2 = \|\mathbf{P}_3 - \mathbf{P}_2\|$ is the distance between two successive points along the path

26

Bild 26

D18 explain, what would be different in 2D and 3D ray-tracing

D.Landskron; 2017-10-03

Water vapour radiometry

- WVR estimate the wet delay by measuring the thermal radiation from the sky
- At microwave frequencies where the atmospheric attenuation due to water vapour is rather high
- WVR do not work during rain or below 15° elevation

Konrad (Elgered et al., 2012)

27

Atmospheric delays for SLR

- Wet part much smaller than for microwaves
- Only modeled, not estimated
- Thus, better estimation of height compared to horizontal components
- Theoretical possibility to estimate troposphere delay with two frequencies, but accuracy of delays not yet sufficient for that

D39

28

Bild 28

D39 just like it is done with the ionosphere
D.Landskron; 2017-10-05

Textbook

- Atmospheric Effects in Space Geodesy, Böhm and Schuh (2013)
- Very detailed description of tropospheric delays

D6 D7

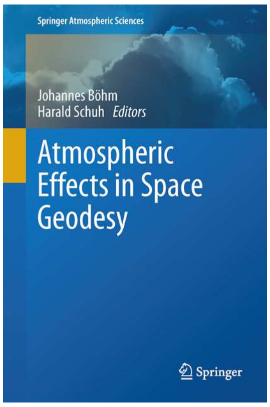

29

3. Vienna Troposphere Models

30

Bild 29

D6 it also describes the physical background of path delays very accurately, which I spared in this presentation for the most part
D.Landskron; 2017-10-03

D7 but, only models before 2013 are considered, that is, no GPT2, GPT3, VMF3, GRAD
D.Landskron; 2017-10-03

Vienna models

- TU Wien has become main provider of troposphere models
- Applicable for GNSS and VLBI analysis
- Included in important software as well as realizations (Bernese, ITRF,..)

31

VLBI

D30

- Plane wavefronts because of huge distance (~10 billion ly)
- Determine phase difference τ between 2 sites
- Correct for errors (ionosphere, troposphere,..)

➔ Station positions and velocities, source positions, zenith wet delay

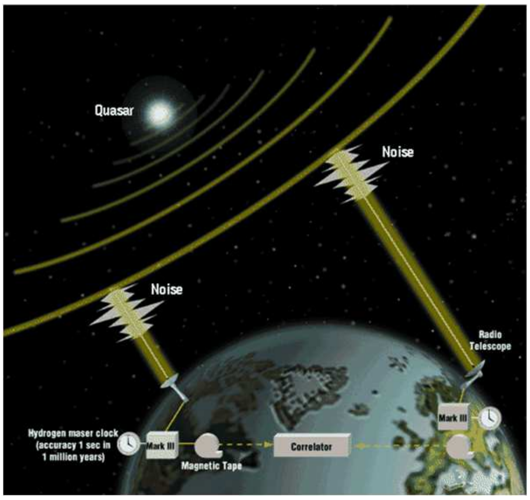

32

Bild 32

D30 I think I do not have to explain GNSS or GPS, but here is a short introduction to VLBI, asI think that not everybody knows about it

D.Landskron; 2017-10-04

Mapping functions

D20

- Discrete mapping functions
  - **VMF**: Vienna Mapping Functions (Böhm and Schuh, 2004)
  - **VMF1**: Vienna Mapping Functions 1 (Böhm et al., 2006)
  - **VMF3**: Vienna Mapping Functions 3 (Landskron and Böhm, 2017)
- Empirical mapping functions
  - **GMF**: Global Mapping Functions (Böhm et al., 2006)
  - **GPT**: Global Pressure and Temperature (Böhm et al., 2007)
  - **GPT2w**: Global Pressure and Temperature 2 (Lagler et al., 2013)
  - **GPT2w**: Global Pressure and Temperature 2 wet (Böhm et al., 2015)
  - **GPT3**: Global Pressure and Temperature 3 (Landskron and Böhm, 2017)
- Hybrid Model
  - **SA-GPT2w**: Site-Augmented GPT2w (Landskron et al., 2015) D21

http://ggosatm.hg.tuwien.ac.at

33

Mapping functions

D24

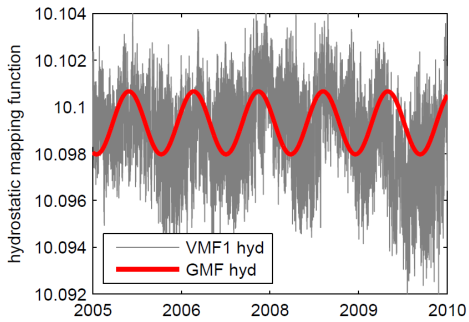

Figure 30: Hydrostatic mapping functions VMF1 and GMF at 5° elevation at Fortaleza, Brazil. Phenomena such as the El Niño event in 2009 cannot be captured with empirical mapping functions like GMF that contain only average seasonal terms

34

Bild 33

D20 Zunächst den Unterschied zwischen discrete und empirical erklären, und dann zu allen Modellen ein paar Wörter sagen
D.Landskron; 2017-10-03

D21 Site-augmentation using in situ meteorological data
D.Landskron; 2017-10-03

Bild 34

D24 D.Landskron; 2017-10-03

Vienna Mapping Functions

- Determined from ray-traced delays through NWM from ECMWF
- Empirical functions for *b* and *c* coefficients
- All information from ray-tracing is condensed into the *a* coefficients
- Available 6-hourly, either at VLBI/GNSS stations or on a global grid D41

35

Vienna Mapping Functions

variable in time and space

$$m(e) = \frac{1 + \frac{a}{1 + \frac{b}{1 + c}}}{\sin(e) + \frac{a}{\sin(e) + \frac{b}{\sin(e) + c}}}$$

ray-tracing

analytical functions

36

Bild 35

D41 the grid is particularly important for GNSS users as they thus can produce zenith delays + mapping functions for any point on Earth

D.Landskron; 2017-10-05

VMF1 vs. VMF3

VMF1	VMF3
b*, *c	***b*, *c***
from 3 years of data on a 10°x10° grid	from 10 years of data on a 2.5°x2.0° grid
lat. dep. for c_h	lat. and lon. dep. for b_h, b_w, c_h and c_w through spherical harmonics (n=m=12)
annual variation for c_h	annual and semi-annual terms for b_h, b_w, c_h and c_w
a	***a***
strictly for el = 3.3°	LSM for el = [3°, 5°, 7°, 10°, 15°, 30°, 70°]
simple 1D ray-tracer	2D ray-tracer “RADIATE” (*Hofmeister*, 2016)

37

Vienna Mapping Functions 3

Spherical harmonics expansion for coefficients *b* and *c* up to degree and order 12

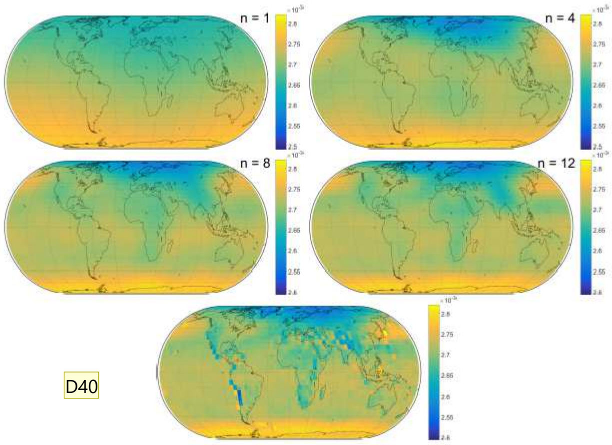

38

Bild 38

D40 and on their basis, new a coefficients were calculated from the ray-traced delays

D.Landskron; 2017-10-05

Global Mapping Functions (GMF)

- GMF: “Averaged” VMF
- Spherical Harmonics up to degree and order 9 for *a*, *b* and *c* from VMF1
- Annual variation with fixed phase (January 28)

$$a = a_0 + A \cdot \cos\left(\frac{\text{doy} - 28}{365.25} \cdot 2\pi\right) ,$$

$$a_0 = \sum_{n=0}^{9} \sum_{m=0}^{n} P_{nm}(sin\theta)(A_{nm}\cos(m\lambda) + B_{nm}\sin(m\lambda))$$

39

Global Pressure and Temperature 2 (GPT2)

- Refined combination of GMF and GPT + additional parameters D25
- Not based on spherical harmonics, but on a grid-wise representation
- Bilinear interpolation from grid to desired location

$$b(t) = A_0 + A_1 \cos\left(\frac{mjd}{365.25} 2\pi\right) + B_1 \sin\left(\frac{mjd}{365.25} 2\pi\right)$$
$$+ A_2 \cos\left(\frac{mjd}{365.25} 4\pi\right) + B_2 \sin\left(\frac{mjd}{365.25} 4\pi\right)$$
$$+ k\, mjd$$

40

Bild 40

D25 GPT2w is actually only a refinement of GPT2 regarding the wet quantities

D.Landskron; 2017-10-03

GPT2w vs. GPT3

GPT2w	GPT3
b*, *c	***b*, *c***
from VMF1	from VMF3
a	***a***
1°x1° or 5°x5° grid	1°x1° or 5°x5° grid
annual and semi-annual terms	annual and semi-annual terms
mf height correction by Niell (1996) for hydr. part	new *mf* height correction for hydr. and wet part
-	horizontal gradients grid
1D ray-tracer	2D ray-tracer "RADIATE" (*Hofmeister*, 2016)
ECMWF monthly means 2001-2010	ECMWF monthly means 2001-2010

41

Global Pressure and Temperature 3

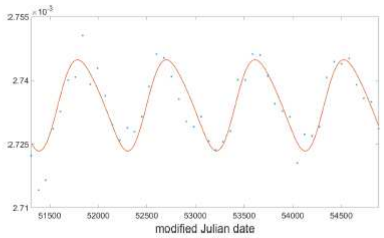

Data fitting in order to derive empirical information

a_h: mean value and annual variation

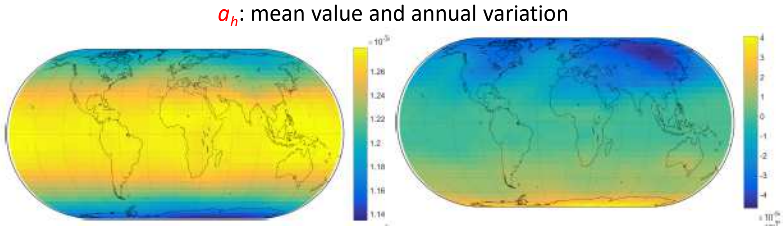

42

Input/output quantities

Table 7 A list of all input and output parameters of the discrete mapping function VMF3

Symbol	Name	Unit
Input parameters		
a_h	Hydrostatic mapping function coefficient	–
a_w	Wet mapping function coefficient	–
mjd	Modified Julian date	–
φ	Geographic latitude	rad
λ	Geographic longitude	rad
zd	Zenith distance (π-elevation)	rad
Output parameters		
mf_h	Hydrostatic mapping factor	–
mf_w	Wet mapping factor	–

Table 8 A list of all input and output parameters of the empirical troposphere model GPT3

Symbol	Name	Unit
Input parameters		
mjd	Modified Julian date	–
φ	Geographic latitude	rad
λ	Geographic longitude	rad
h_{ell}	Ellipsoidal height	m
Output parameters		
p	Pressure	hPa
T	Temperature	°C
dT	Temperature lapse rate	K km^{-1}
T_m	Mean temperature weighted with water vapor pressure	K
e	Water vapor pressure	hPa
a_h	Hydrostatic mapping function coefficient (valid at sea level)	–
a_w	Wet mapping function coefficient	–
λ	Water vapor decrease factor	–
N	Geoid undulation	m
G_{n_h}	Hydrostatic north gradient	m
G_{e_h}	Hydrostatic east gradient	m
G_{n_w}	Wet north gradient	m
G_{e_w}	Wet east gradient	m

43

Handling for user

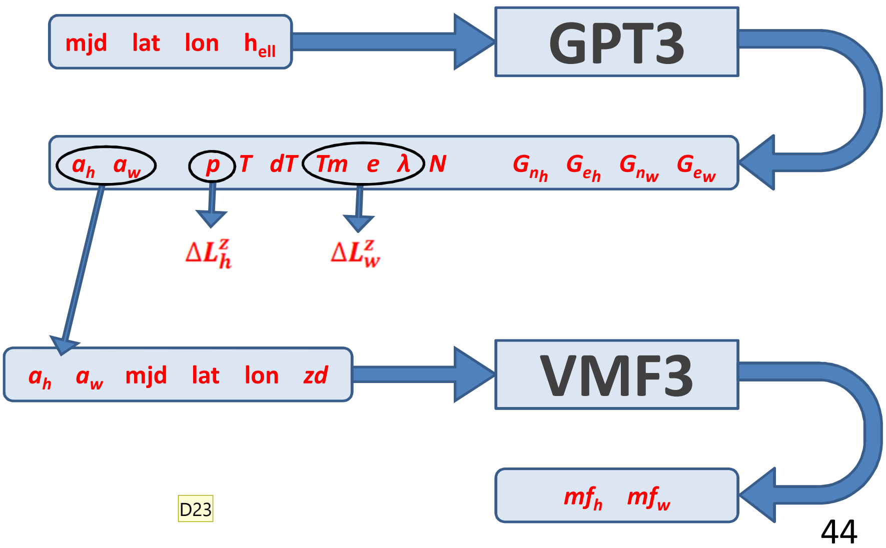

D23

44

Bild 44

D23 so we see that GPT3 acts as a complete troposphere model which outputs all information that may be required in troposphere modeling

D.Landskron; 2017-10-03

Mapping functions comparison

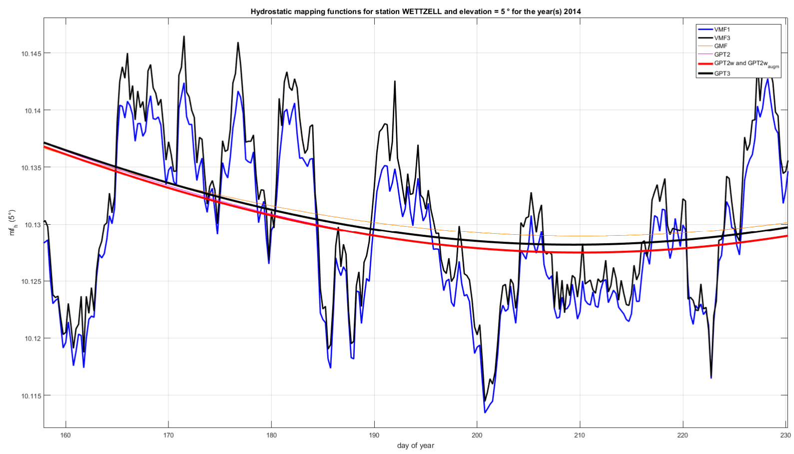

45

Mapping functions comparison

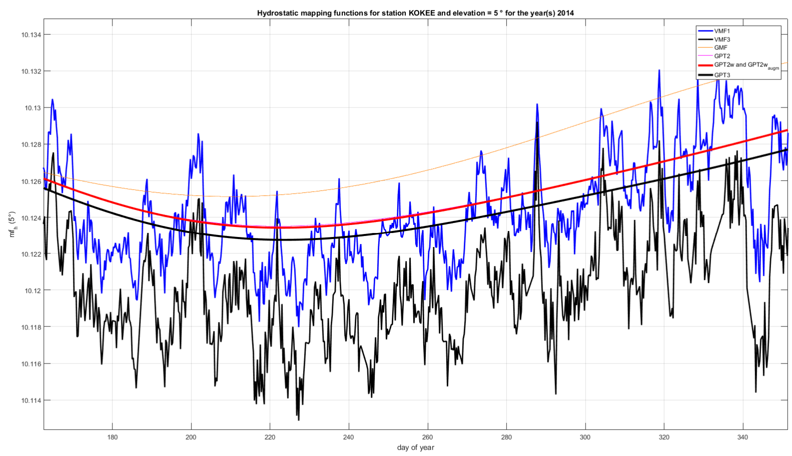

46

Delay comparison

Differences in slant total delay to ray-tracing (mm)
2592 grid points
120 epochs (2001-2010)
el = 5°

VMF1 **VMF3**

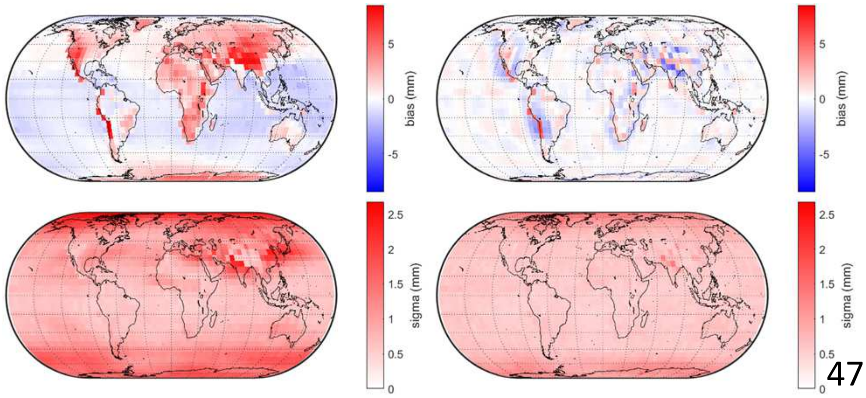

47

Delay comparison

Differences in slant total delay to ray-tracing (mm)
2592 grid points
120 epochs (2001-2010)
el = 5°

GPT2w **GPT3**

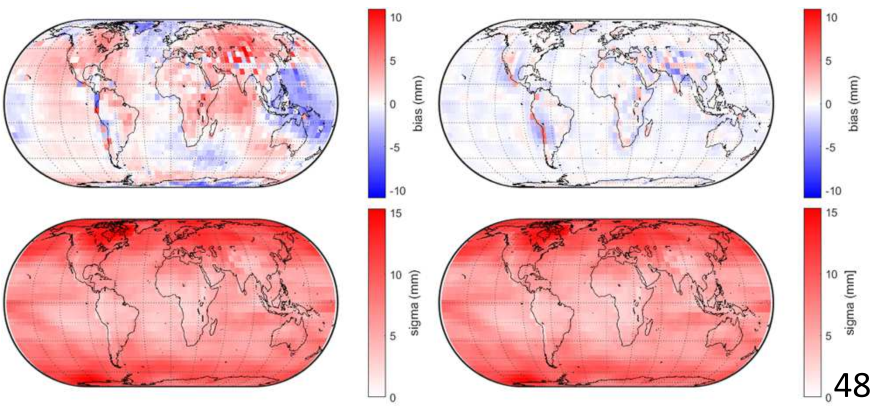

48

Delay comparison

Mean absolute error (MAE) in slant delay w.r.t. ray-tracing (mm)
2592 grid points
120 epochs (2001-2010)
el = 5°

(mm)	ΔL	ΔL_h	ΔL_w
VMF1	**1.73**	1.67	0.30
VMF3	**0.82**	0.73	0.30
GPT2w	**6.85**	6.10	1.63
GPT3	**6.46**	5.68	1.60

49

Delay comparison

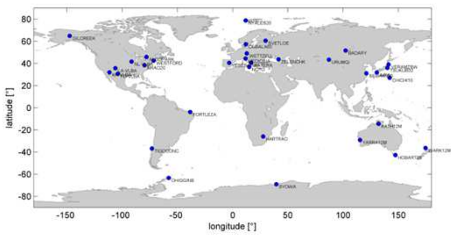

Mean absolute diff in slant total delay w.r.t. ray-tracing (mm)
33 sites around the world
1999-2014

D32

[mm]	3°	5°	7°	10°
VMF1	0.52	3.98	2.54	1.47
VMF3	1.17	2.64	1.66	0.91
GPT2w (1°x1°)	54.13	18.95	8.35	3.27
GPT3 (1°x1°)	53.68	18.90	8.30	3.24

50

Bild 50

D32 there is a lot of information in this plot: auf alles eingehen

D.Landskron; 2017-10-04

Delay comparison

Mean difference w.r.t. ray-tracing (mm)
33 sites around the world, 1999-2014, el =5°

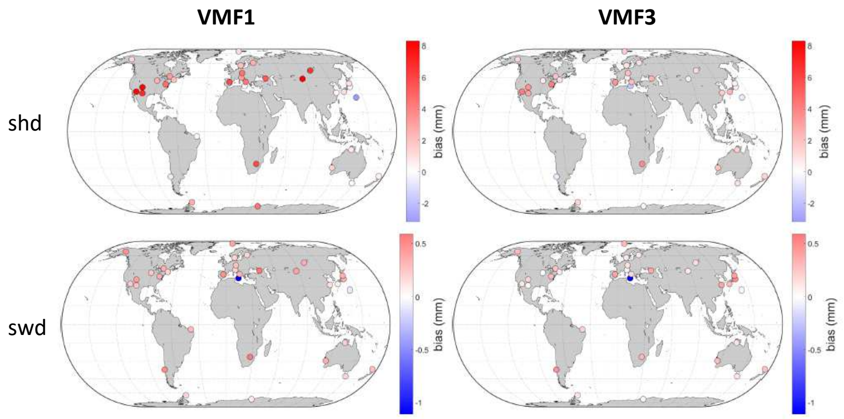

51

BLR comparison

- Baseline Length Repeatability (BLR) from VLBI analysis good tool for assessing accuracy of geodetic products
- Analysis with Vienna VLBI and Satellite Software (VieVS) D33
- Hardly any difference between the mapping function models D34
- Main influence from zenith delays, mapping functions not that effective
- Estimation of zenith wet delays very accurate

52

Bild 52

D33 if somebody is interested in learning how to use VieVS as a VLBI analysis softwase
D.Landskron; 2017-10-04

D34 not even between empirical and discrete models
D.Landskron; 2017-10-04

Site-augmented GPT2w

1. Empirical ΔL_w^z from GPT2w
2. Measure T and e in situ
3. Augment the empirical ΔL_w^z

$$zwd = zwd_{GPT2w} + M_1 * (T_{in\ situ} - T_{GPT2w}) + M_2 * (e_{in\ situ} - e_{GPT2w})$$

53

Site-augmented GPT2w

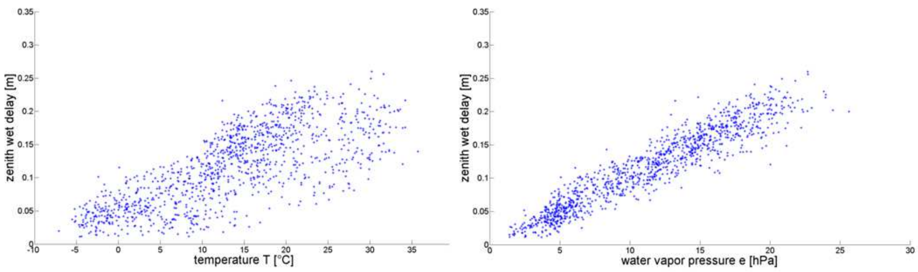

T with ΔL_w^z: 0.65 e with ΔL_w^z: 0.85

$$zwd = zwd_{GPT2w} + M_1 * (T_{in\ situ} - T_{GPT2w}) + M_2 * (e_{in\ situ} - e_{GPT2w})$$

Universal, global coefficients M_1, M_2:
M_1 = **4.9 * 10^{-4}** [m/°C^{-1}]
M_2 = **0.00915** [m/hPa^{-1}]

54

Site-augmented GPT2w

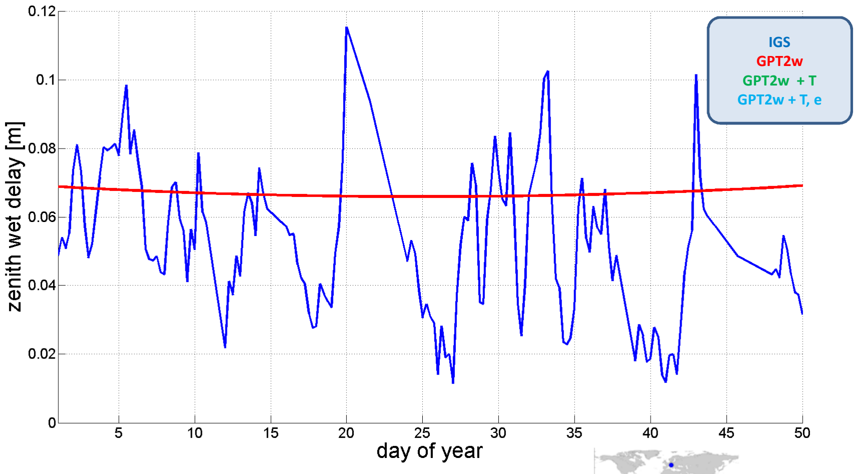

Comparison of ΔL_w^z for **BZRG**

Site-augmented GPT2w

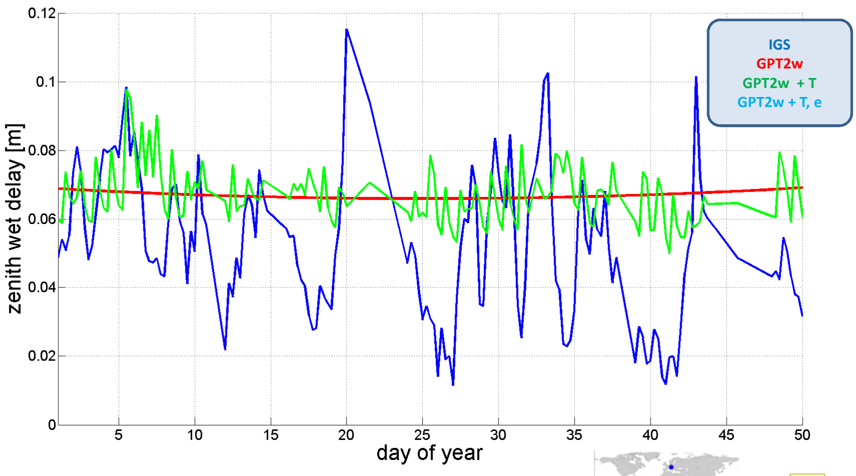

D35

Comparison of ΔL_w^z for **BZRG**

Bild 56

D35 when measuring T,we get the green line which is already slightly closer to the real data
D.Landskron; 2015-10-14

Site-augmented GPT2w

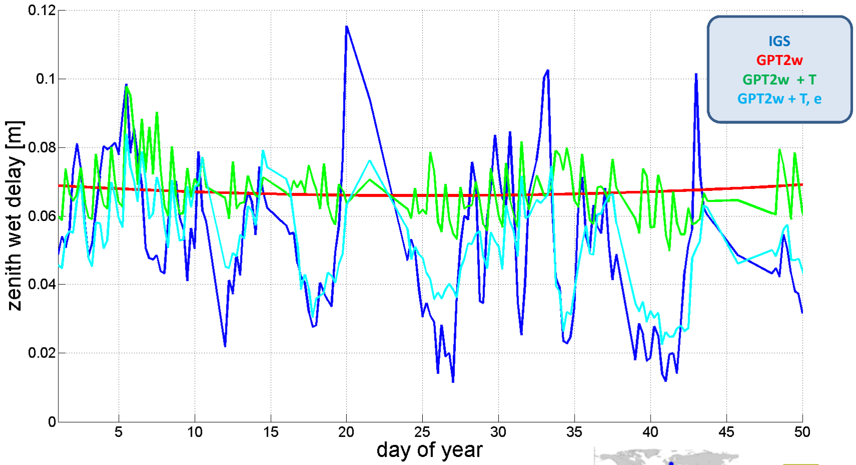

D36

Comparison of ΔL_w^z for **BZRG**

Site-augmented GPT2w

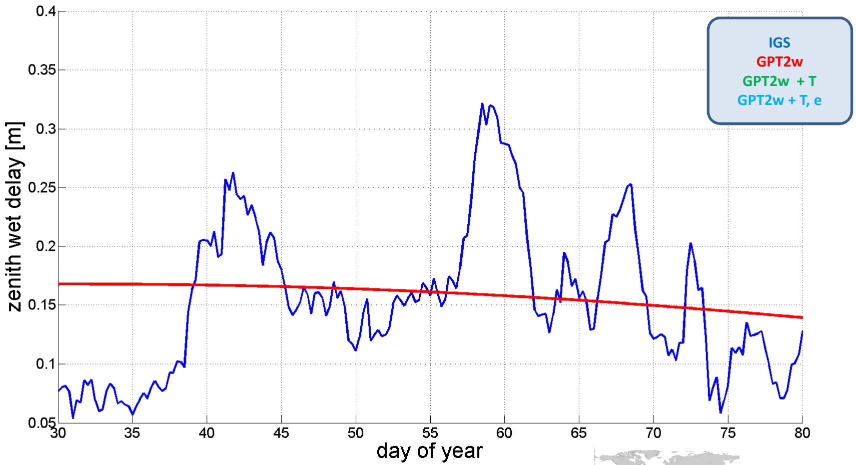

Comparison of ΔL_w^z for **ALIC**

Bild 57

D36 when also measuring water vapor pressure, then the maximum improvement is achieved
D.Landskron; 2015-10-14

Site-augmented GPT2w

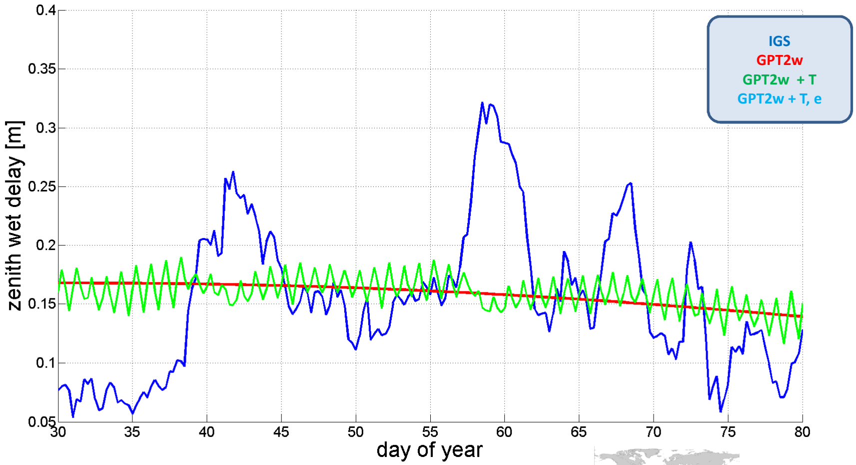

Comparison of ΔL_w^z for **ALIC**

Site-augmented GPT2w

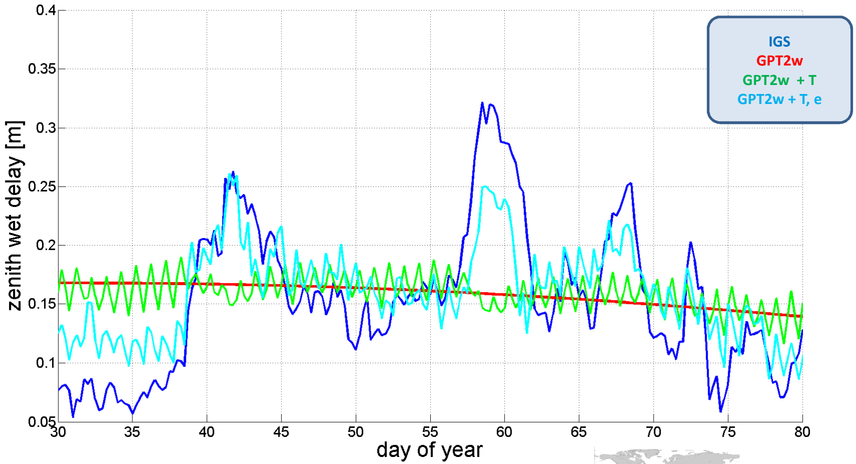

Comparison of ΔL_w^z for **ALIC**

Site-augmented GPT2w

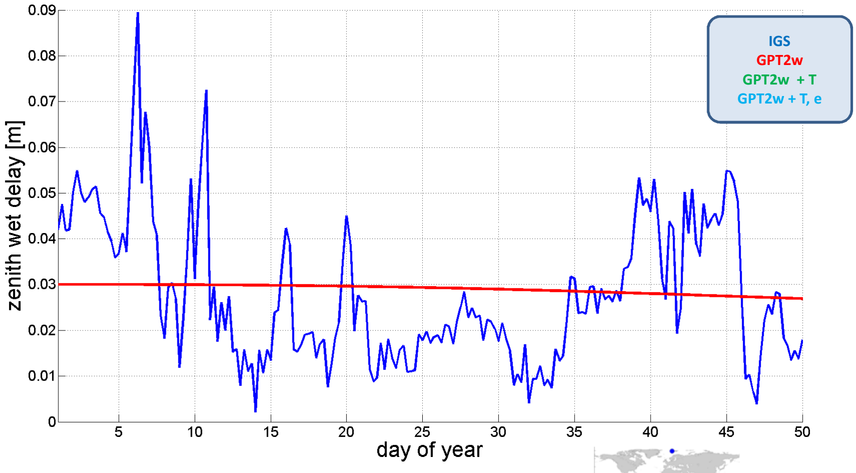

Comparison of ΔL_w^z for **NYA1**

2016/02/10

Refined and site-augmented tropospheric delay models for GNSS applications (Landskron et al., 2016)

61

Site-augmented GPT2w

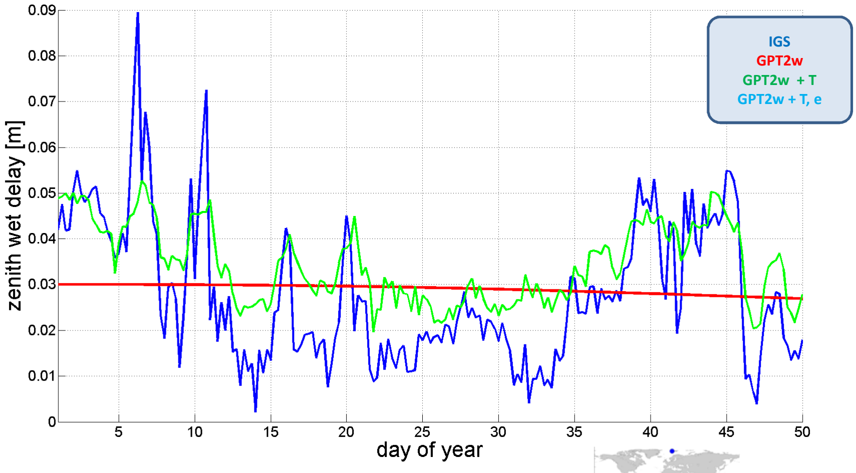

Comparison of ΔL_w^z for **NYA1**

2016/02/10

Refined and site-augmented tropospheric delay models for GNSS applications (Landskron et al., 2016)

62

Site-augmented GPT2w

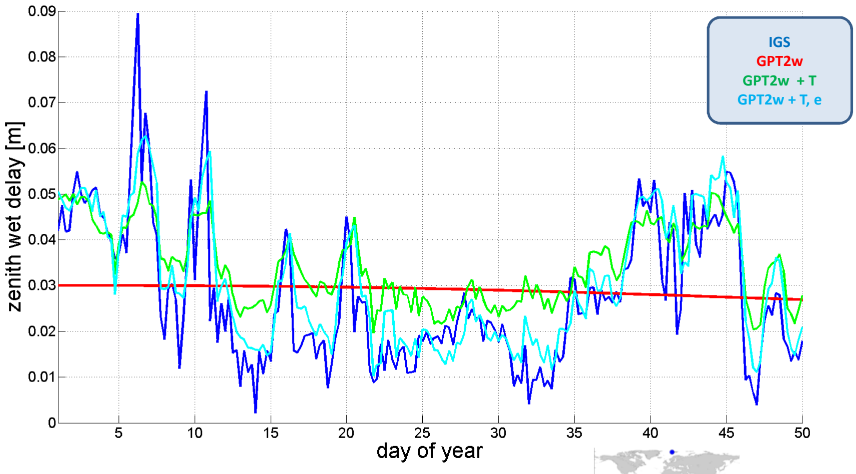

Comparison of ΔL_w^z for **NYA1**

Refined and site-augmented tropospheric delay models for GNSS applications (Landskron et al., 2016)

Site-augmented GPT2w

Mean absolute error (MAE) in zenith wet delay to ray-tracing (cm)
33 sites around the world
1999-2014

(cm)	zwd
GPT2w	2.8
GPT2w+ *T*	2.7
GPT2w+ *T* and *e*	2.0

Site-augmented GPT2w

- GPT2w well suited for site-augmented approach using in situ measurements of *T* and *e*
- in situ measurement of *T* yields small improvement in zenith wet delay ΔL_w^z (~5%)
- additional in situ measurement of *e* yields significant improvement in zenith wet delay ΔL_w^z (~30%)
- In general, best performance of site-augmented GPT2w is achieved in dry regions

Horizontal gradients

D22

- Discrete a priori gradient models
  - **LHG**: Linear Horizontal Gradients (Böhm and Schuh, 2007)
  - **GRAD** (Landskron et al., 2016)
- Empirical a priori gradient models
  - **APG**: A priori gradients (Böhm et al., 2013)
  - **GPT3**: Global Pressure and Temperature 3 (Landskron and Böhm, 2017)

http://ggosatm.hg.tuwien.ac.at

Bild 66

D22 the list of a priori gradient models is less comprehensive, because very often such models are not used in analysis at all, as the gradients are estimated in the data analysis though least-squares adjustment

D.Landskron; 2017-10-03

A priori gradients GRAD

D26

- Determined from 2D-raytracing at 7 elevations and 16 azimuths through LSM
- For all VLBI measurements
- 6-hourly (at each NWM epoch)

$$\Delta L(a,e) = \Delta L_0(e) + mf_g(G_n \cos a + G_e \sin \mathrm{a})$$ **= GRAD-1**

$$\Delta L(a,e) = \Delta L_0(e) + mf_g\big(G_n \cos a + G_e \sin \mathrm{a} + G_{n_2} \cos 2a + G_{e_2} \sin 2\mathrm{a}\big)$$ **= GRAD-2**

67

A priori gradients GRAD

Residuals between ray-traced delays and modeled delays

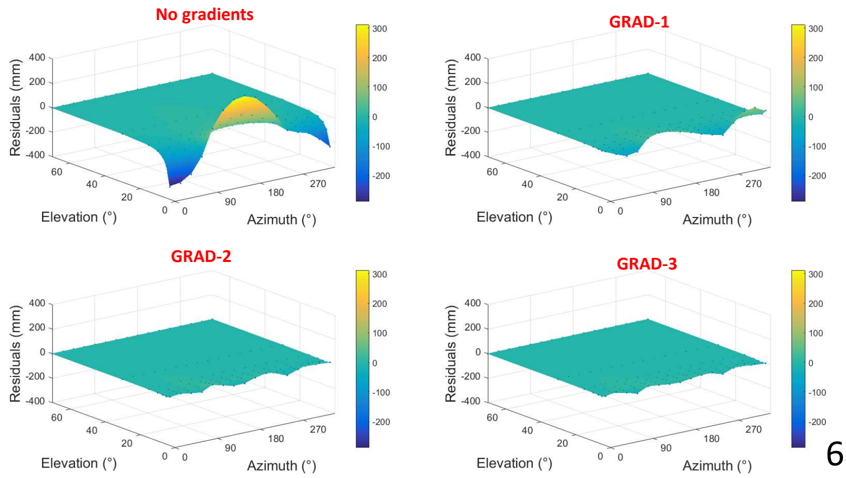

68

Bild 67

D26 the most precise a priori gradients available are the gradients GRAD. They are splitted into 3 versions, depending on three different gradient formulas, with GRAD-1 being the main model however

D.Landskron; 2017-10-03

A priori gradients GRAD

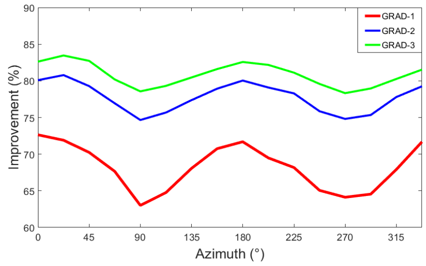

Higher-order gradients improve delays
WETTZELL, September 2011

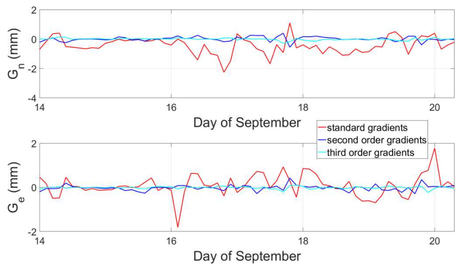

Higher-order gradients smaller in size
WETTZELL, September 2011

```
#
#   (1)       (2)       (3)    (4)    (5)    (6)    (7)      (8)      (9)     (10)
# station |   mjd    | Gn_h | Ge_h | Gn_w | Ge_w | Gn2_h  | Ge2_h  | Gn2_w  | Ge2_w
#
TSUKUB32  57388.25  -0.384 -0.313  0.047  0.060 -0.009  0.048 -0.014 -0.003
WETTZELL  57388.25  -0.273 -0.080 -0.235  0.107 -0.071  0.018 -0.000  0.015
TSUKUB32  57388.50  -0.325 -0.263 -0.063 -0.057 -0.005  0.037  0.008 -0.001
WETTZELL  57388.50  -0.258 -0.216 -0.054 -0.075 -0.021 -0.025 -0.004 -0.021
TSUKUB32  57388.75  -0.431 -0.229 -0.060  0.064 -0.018  0.028 -0.041 -0.004
WETTZELL  57388.75  -0.204 -0.206  0.034 -0.147 -0.074 -0.001  0.006  0.007
```

69

Global Pressure and Temperature 3 (GPT3)

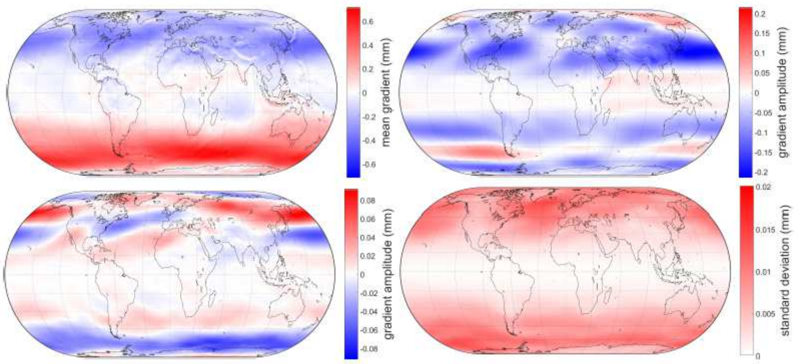

Fig. 3 Mean values A_0 (top left), annual amplitudes A_1 (top right), semi-annual amplitudes A_2 (bottom left) and standard deviation of the residuals (bottom right) of the hydrostatic north gradient G_{n_h} from GPT3.

70

Global Pressure and Temperature 3 (GPT3)

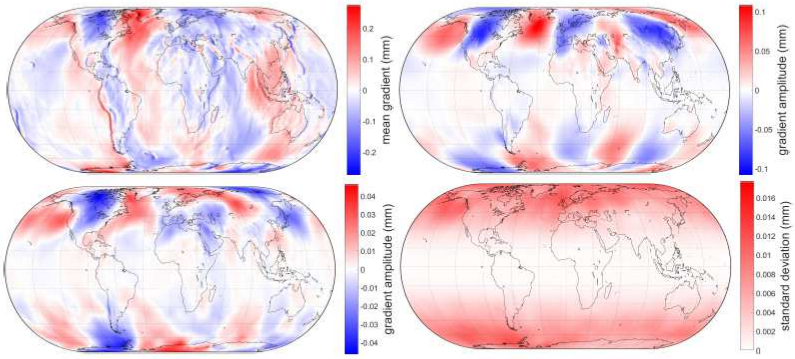

Fig. 4 Mean values A_0 (top left), annual amplitudes A_1 (top right), semi-annual amplitudes A_2 (bottom left) and standard deviation of the residuals (bottom right) of the hydrostatic east gradient G_{e_h} from GPT3.

71

Gradient comparison

Empirical gradients only describe a fraction of the real gradients

WETTZELL, 06/2014–12/2014

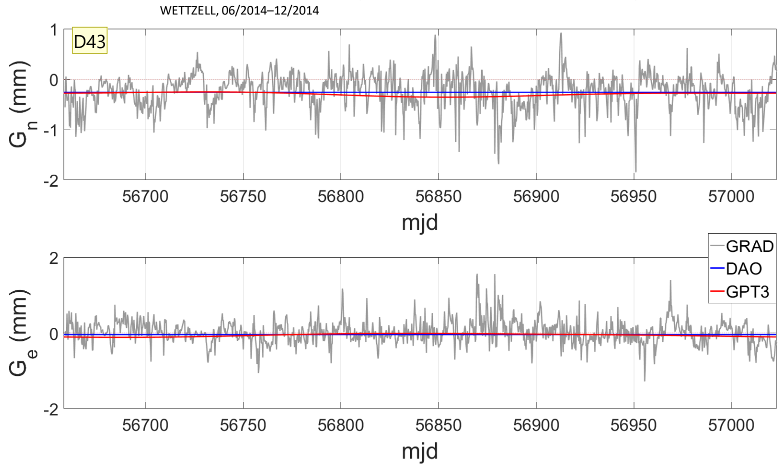

72

Bild 72

D43 D.Landskron; 2017-10-05

Gradient comparison

Mean absolute residuals (mm) between ray-tracing and VMF3 + gradient models at el = 5°

Gradient Model	Mean Abs. Diff. in ΔL (cm)					
	$\alpha = 0°$	$\alpha = 45°$	$\alpha = 90°$	$\alpha = 135°$	$\alpha = 180°$	mean α
no a priori gradients	25.6	19.6	9.7	19.0	26.0	**20.0**
GRAD-1	4.1	1.1	4.1	1.1	4.2	**2.9**
GRAD-2	1.4	0.8	1.1	0.8	1.3	**1.1**
GRAD-3	1.4	0.8	1.1	0.8	1.3	**1.1**
APG	16.4	14.4	10.8	13.0	16.8	**14.3**
GPT3	9.4	7.5	7.4	7.5	9.5	**8.3**

73

Gradient comparison

Baseline length repeatability (BLR) from 1338 VLBI sessions from 2006-2014

(cm)	NO estimation	WITH estimation
Ray-tracing	1.57	1.64
No a priori gradients	1.68	1.65
LHG	1.66	1.67
GRAD-1	1.58	1.66
GRAD-2	**1.57**	**1.65**
DAO	1.64	1.66
GPT3	1.63	1.66

74

Gradients results

- GRAD yield best performance of all a priori gradients
- Use of a priori gradients in VLBI analysis is very important
- Estimation only makes sense when enough observations
- Empirical gradients may be valuable for GNSS D38

75

4. Conclusions

76

Bild 75

D38 Because they can be produced for any point on Earth
D.Landskron; 2017-10-04

Conclusions

- Many troposphere models from TU Wien
- Mapping functions + horizontal gradients
- Applicable for GNSS and VLBI analysis
- VMF1 and GMF most important ones
- Ray-tracing through NWM best approach

D42

77

Conclusions

- Several new/refined models created
  - Mapping functions + horizontal gradients
  - All of which outperform predecessors, but only to a small degree
- Tropospheric modeling close to peak of technical means?
  - (Reference) ray-traced delays approximated very well
  - Denser and more accurate NWM
  - Improved strategies and concepts

78

Bild 77

D42 yielding accuracies which by far surpassed those from before
D.Landskron; 2017-10-05

5. Outlook

Outlook

- Operationally provide VMF3/GRAD
  - for all IVS stations (VLBI)
  - for all IGS stations (GNSS)
  - for all IDS stations (DORIS)
  - on a grid
  - for Satellite Laser Ranging (SLR)
- Distribute all data via:

D4

http://ggosatm.hg.tuwien.ac.at

Bild 80

D4 and in future from a new server

Daniel; 2017-10-14